RANKINE CYCLE POWER AUGMENTATION: ORC AND ABSORPTION CHILLER

Vitor R. Seifert, vitor.seifert@ufba.br
Yuri M. Barbosa, yuri_mbarbos@hotmail.com
Federal University of Bahia, Industrial Engineering Program. Rua Aristides Novis, 2. CEP 40210-630, Federação, Salvador, Bahia, Brazil

Júlio A. M. da Silva, julio.silva@ufba.br
Federal University of Bahia, Department of Mechanical Engineering, Salvador, Bahia, Brazil

Ednildo A. Torres, ednildotorres@gmail.com
Federal University of Bahia, Department of Chemical Engineering, Salvador, Bahia, Brazil

Abstract. *The search for more efficient processes in order to save resources and avoid further environmental damages is mandatory in current society. Increases in power and efficiency of already existing power plants play important role in the transition to more efficient cycles. This work compares two different thermal arrangements that can be fitted in already existing Rankine cycle power plants to improve their power and efficiency. These arrangements are possible when fuel sulfur concentration is reduced to meet SOx emission legislation. The first thermal arrangement is composed of an absorption chiller and a chilled water storage tank designed to make use of the energy remaining in boiler exhaust gases. Thermal accumulation enables the use of chilled water generated during the period of 24 hours by the absorption chiller. This chilled water can be used in the condenser during peak hours to increase power output and the efficiency of the plant. The second option is fitting an Organic Rankine Cycle (ORC) powered by the waste heat of the exhaust gases from the boiler. Results show that fitting an ORC using n-Butane as a working fluid represents a gain of 409.3 kW on net power and 0.42% on efficiency against 55.92 kW and 0.07% gained by using the absorption chiller. Therefore it is more interesting to apply an ORC than an absorption chiller to the existing power plants operating under the same conditions.*

Keywords*: repowering, Rankine cycle, power plant, absorption chiller, ORC*

1. INTRODUCTION

The search for renewable energy sources and increasing energy efficiency in power generation has been a common concern in recent years. Also, there is a concern over emissions of greenhouse gases like CO_2 from fossil fuel combustion. Some studies aim to increase that efficiency and consequently reduce the usage of fossil fuel to generate electrical energy. Many power generation plants are based on Rankine cycles, gas turbines (Brayton cycle) or alternative engines (Otto/Diesel). The efficiency of these systems may be increased by using absorption chillers or Organic Rankine cycles (ORC) powered by the waste heat of the exhaust gases from the cycles.

The use of cooling equipments to enhance the power generation is common in the literature. The performance of gas turbines for example is dependent on ambient temperature (Kim and Ro, 2000). The most common application for these systems is reducing turbine inlet air temperature in order to increase the mass quantity of air that enters the equipment (Celis et al., 2007). Shirazi et al. (2014) presented a mathematical model for an ice thermal energy storage (ITES) system applied to cool a gas turbine inlet air. It was concluded that using ITES to cool the inlet air would result in an improvement of 11.63% on power output and 3.59% on the exergetic efficiency. The efficiency of a Rankine Cycle power plant depends on the condensation temperature. The reduction of this temperature decreases the condensation pressure, which means more power output on the expansion in the turbine and consequently greater cycle efficiency. A particular plant may have an increase of around 10% in power generation when the condenser pressure is changed from 0.087 bar to 0.033 bar (Agnew et al., 2004). Muñoz et al., (2011) analyzed the performance of a Rankine cycle in which the energy from the exhausting gases of the boiler was used to feed an absorption chiller in order to chill the condenser cooling water. The conclusion was that the cycle exhausting gases cannot provide enough energy for this purpose. The authors proposed the use of a cold water storage tank to keep the water cooled by the absorption chiller cold. This water would be used during peak consumption hours to increase the power produced by the Rankine cycle. This configuration will be analyzed in this work.

Recently ORCs have been studied due to their ability to use low-grade heat sources like waste heat from industry, geothermal energy and solar energy to produce electricity (Calise et al., 2015). ORCs are more interesting than conventional Rankine cycles which use water/steam as a working fluid because of the better adaptation of organic fluid properties in dealing with low temperature heat sources. Some of the beneficial properties are the positive inclination of vapor saturation line and proper condensation and evaporation pressure under the temperatures of the environment and the heat sources, respectively, for turbine expansion. The use of organic fluids also results in more compact system and reduces the costs of implementation and maintenance of the system (Rahbar et al., 2015). Song et al. (2015) analyzed an

ORC to recover waste heat from marine diesel engines using jackets cooling water and the exhaust gases to obtain maximum power output. A cycle that used the jackets cooling water to pre-heat the working fluid and the exhaust gases to evaporate it resulted in a gain of 99.7 kW in power generation with low implementation costs. Galindo et al. (2015) analyzed thermodynamically and experimentally an ORC using waste heat from a gasoline engine. Other authors like Shu et al. (2014) and Battista et al. (2015) also studied the effects of the operational characteristics on the performance of ORCs attached to combustion engines. The first concluded that azeotropic mixtures of organic fluids result in lower efficiencies than most pure organic fluids with great exergy loss, while zeotropic mixtures in certain proportions result in higher efficiency and lower exergy losses compared to the same pure organic fluids. The second concluded that the installation of an ORC to a conventional gasoline engine with turbo-compressor can increase the mechanical efficiency of the system in up to 3.7%.

Chacartegui et al. (2009) analyzed the applicability of ORC cycles to use the exhaust gases from regenerative gas turbines. This configuration compared to conventional gas turbines result on exhaust gases at lower temperatures which can be used as heat source to generate vapor for the ORC. The optimization was conducted based on turbine inlet temperature and resulted in a gain of efficiency superior to the combined cycles presented on the literature. Clemente et al. (2013) study was focused on the application of an ORC cycle to use exhaust gases from small scale gas turbines (100 kWe). Comparing the options for the ORC expanders the author concluded that single stage turbines are more advantageous than positive displacement expanders because the first can be connected to the gas turbine shaft as well as result in higher gains of efficiency to the cycle. For this application refrigerant fluids are more interesting because they allow the use of compact equipments. Camporeale et al. (2015) analyzed thermodynamically and technical-economically an ORC using waste heat from the exhaust gases from a non-regenerative gas turbine powered by biomass combustion. The absence of a regenerator results in higher temperature of the exhaust gases. It was concluded that superheating on subcritical ORCs causes efficiency losses. Therefore it is preferable to use cycles with evaporation close to the saturation line. The same issue was observed for supercritical cycles. Therefore the ideal is to keep the parameters next to the critical point. For this specific application the most-suitable fluid is the Toluene due to the higher heat recovery rate. The economical analysis showed that the simple application of an ORC makes the generation of electricity more profitable. However, if the price and the need of thermal energy were high it could be more advantageous to sell thermal energy instead of generating electricity with the ORC. Chacartegui et al. (2015) studied the application of an ORC to use exhaust gases from a Humid Air Turbine for distributed micro-generation. Results show a gain of 25% on power generated which corresponds to an increase of 11% on the efficiency when compared to an isolated gas turbine. The economical analysis showed a reduction of 15% on the cost of electricity which indicates that this application is promising for this specific case due to its simplicity and cost.

In this work the ORC makes use of the opportunity created when the fuel used in a boiler is replaced by a fuel with lower sulfur concentration, therefore the energy remaining in exhausting gases can be further used without acid condensation. An optimization procedure is performed in order to find the cycle configuration which provides maximum power output for each tested fluid. The result of the ORC proposal is compared to the results from the thermal scheme using energy storage and an absorption chiller to chill condenser cooling water.

2. SYSTEM MODELING

For this work a typical Rankine cycle is used. The following sub topics present some simplifying assumptions, the characteristics of the typical Rankine cycle and the proposed changes in order to increase both power generation and cycle efficiency.

2.1 Simplifying assumptions

1. Changes in potential and kinetic energies are considered negligible.
2. All components operate under steady state condition except for the chilled water tank.
3. The pressure drop in pipeline is disregarded.
4. Environment temperature and humidity remains constant along the analysis.

2.2 Studied Rankine Cycle

This analysis is carried out considering the Rankine cycle shown in Figure 1.

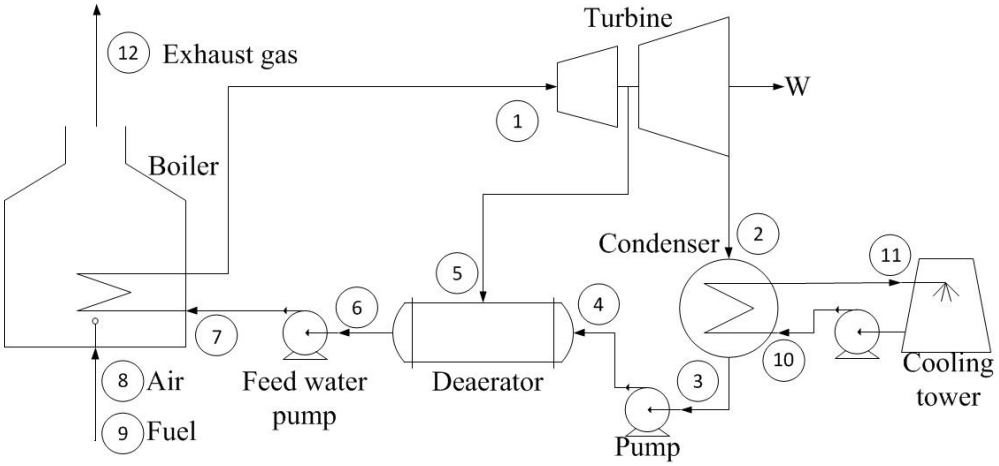

Figure 1. Studied Rankine cycle

The boiler produces 27,78 kg/s of steam at 485ºC and 9100 kPa. Exhaust gases leave at 175,6ºC. Saturated steam enters in condenser at 45ºC, while the water exits the cooling tower at 30ºC and returns at 40ºC. The temperature and pressure of the subcooled liquid in the output of deaerator are respectively 133ºC and 300 kPa. All pumps have isentropic efficiency of 80%. The turbine has isentropic efficiency of 85% and the boiler has thermal efficiency of 92%. Table 1 and Table 2 show respectively the properties of each stream of the cycle and the calculated global data.

Table 1. Studied Rankine cycle thermodynamic properties

Stream	Mass flow (kg/s)	Pressure (kPa)	Temperature (ºC)	Quality	Enthalpy (kJ/kg)	Entropy (kJ/kgK)
1	27.78	9100.0	485.00	----	3347.86	6.6038
2	23.68	9.6	45.00	0.83	2175.98	6.8858
3	23.68	9.6	45.00	0.00	188.44	0.6388
4	23.68	300.0	45.05	----	188.85	0.6392
5	4.10	300.0	133.53	0.98	2684.31	6.8918
6	27.78	300.0	132.53	----	557.19	1.6614
7	27.78	9,100.0	133.93	----	569.05	1.6674
8	33.97	101.3	25.00	----	----	----
9	2.08	101.3	25.00	----	----	----
10	1,126.93	229.5	31.00	----	143.86	0.4306
11	1,126.93	200.0	40.00	----	185.17	0.5646
12	35.73	101.3	175.61	----	187.77	0.7600

Table 2. Calculated global data of the studied Rankine cycle

Global Data	Value	Unit
W_{tot_gross}	30.47	[MW]
W_{net}	30.13	[MW]
η_{cycle}	35.91	[%]
Heat Rate	10,025.16	[MJ/MWh]
Back Work Ratio	1.11	[%]

2.3 Exhausting gases acid dew point

According to Ganapathy (1994), if the temperature of the exhausted gases reaches the acid dew point temperature, corrosion problems may occur. It is a general trend nowadays the replacement of sulfur rich fuels by fuels with lower concentration of this element in order to avoid excessive SO_x emissions. The most known example is the gradual replacement of S1800 diesel by S10 diesel in Brazil in the last decades. This kind replacement also allows further use of exhausting gases energy, since the dew point of these gases will be lowered due to the reduced sulfur content. Table 3 shows some comom used fuel, their composition and dew point. Fuel oil 1 A was selected due to its lower amount of sulfur as the substitute to the used fuel which allows 175,6ºC as exhausting temperature.

Table 3. Fuels studied in this work

Fuel	C	H	S	Other elements	LCV (MJ/kg)	Acid dew point (ºC)[1]
Oil 1A	85.20	10.80	0.04	3.96	40.43	101.49
Oil 2B	87.30	11.10	0.74	0.86	41.08	129.03
Oil 1B	85.60	11.30	0.80	2.30	41.16	130.10
Oil 2A	85.30	10.40	2.80	1.50	39.97	142.14

2.4 First proposal: Absorption chiller

In this proposal an absorption chiller is fitted in the Rankine cycle using the boiler exhaust gases as heat source. During the operation of the cycle, the chiller cools water and directs it into the cold water storage tanks. At peak electricity consumption, the stored cold water is drained into the condenser, replacing the cooling water from cooling tower. The cold water reduces the condensation pressure increasing the enthalpy variation through the turbine and resulting in greater power output and efficiency. Figure 2 shows the proposed system.

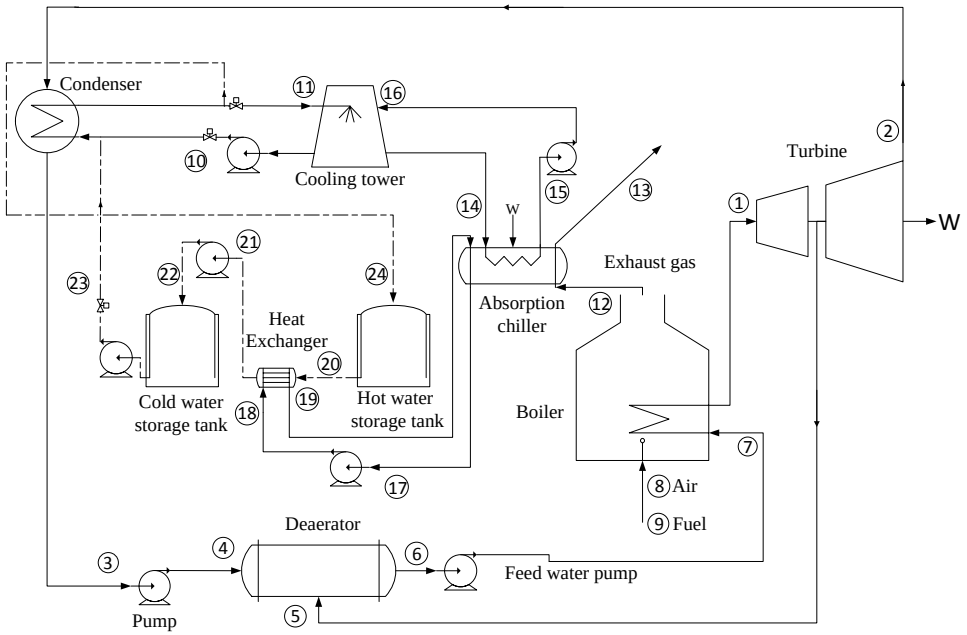

Figure 2. Proposed Rankine cycle with absorption chiller

2.4.1 Standard operation mode

Under standard mode the Rankine cycle operates according to Fig.1. The condenser is cooled by the cooling tower water and the absorption chiller cools the water stored in the hot water storage tank. This cold water is stored into the cold water storage tank. When the cold water tank is full, the cycle is ready to operate in repowering mode.

2.4.2 Repowering operation mode

Under repowering mode the water flow from the cooling tower is blocked and the cold water from the tank is drained into the condenser and returns to the hot water storage tank. The mass flow rate needed to cool the condenser is considerably greater than the flow rate of cold water that the absorption chiller can provide. Therefore, this repowering operation mode only occurs for a short period of time.

2.4.3 Determination of the repowering operation time

During repowering mode cold water is drained into the condenser with mass flow rate $\dot{m}_{resf}$ while the cold water storage tank receives water cooled by the chiller with mass flow rate $\dot{m}_{chiller}$. The duration of the repowering mode t_R is determined by:

$$M_{water} = \left(\dot{m}_{resf} - \dot{m}_{chiller}\right) * t_R \quad (1)$$

M_{water} is the tank capacity in mass (kg). After the full discharge of cold water, the cycle restarts to operate in standard mode during a period of time t_S.

$$M_{water} = \dot{m}_{chiller} * t_S \tag{2}$$

For the proposed system it is required a tank whose capacity is 2915.29 m³. Considering that the tank diameter is equal to its height both values are 15.48m.

2.4.4 Condenser analysis

During standard operation the heat rejected by the condenser $\dot{Q}_{rej}$ is determined by Eq. (3) and Eq. (4):

$$\dot{Q}_{rej} = U_C * A_C * \Delta T_{ml} \tag{3}$$

$$\dot{Q}_{rej} = \dot{m}_w * \Delta h_{Cond} \tag{4}$$

U_C is the overall heat transfer coefficient here considered as 2,5 kW/m²K (Kakaç, 2002). A_C is the total area of thermal exchange. $\dot{m}_w$ is the mass flow rate of working fluid whose condensation enthalpy is Δh_{Cond}. ΔT_{ml} is the logarithmic mean temperature difference of the streams on the condenser. The calculated thermal exchange area of the condenser was 2068 m². Figure 3a shows the arrangement for the condenser during standard operation mode.

During repowering operation the heat rejected by the condenser is calculated iteratively by Eq. (5), Eq. (6) and Eq. (7). $\dot{m}_{w\_rep}$ is the working fluid mass flow rate for the repowering operation mode, C_p is the specific heat of the water and ΔT_{23-20} is the temperature difference between streams 20 and 23 shown in Fig. 3b.

$$\dot{Q}_{rej} = U_C * A_C * \Delta T_{ml} \tag{5}$$

$$\dot{Q}_{rej} = \dot{m}_{w\_rep} * \Delta h_{Cond} \tag{6}$$

$$\dot{Q}_{rej} = \dot{m}_{resf} * Cp * \Delta T_{23-20} \tag{7}$$

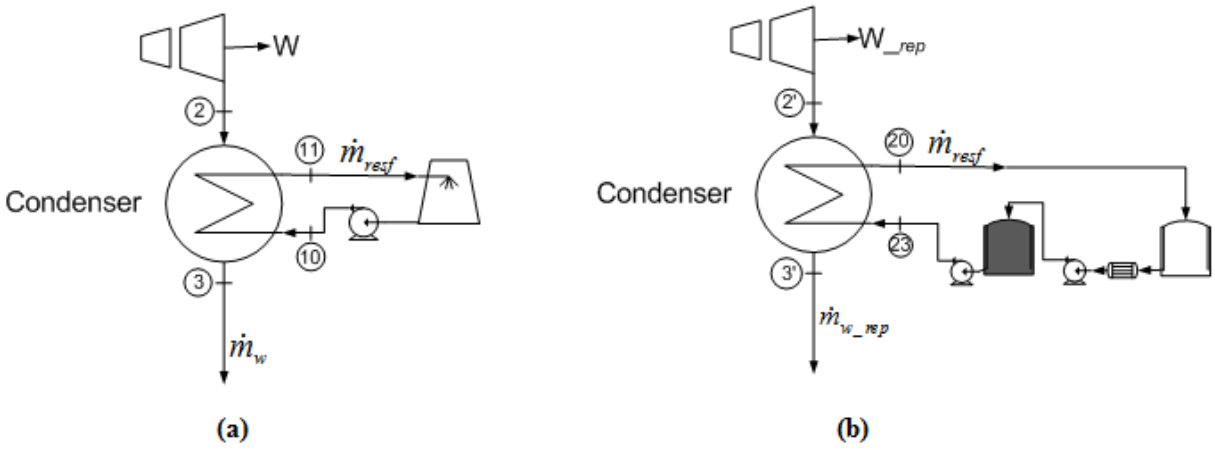

Figure 3. Arrangement for the condenser: (a) Standard operation mode, (b) Repowering operation mode.

2.4.4 Results

During repowering operation the condensation temperature decreases resulting in less heat rejected to the ambient. Therefore the cycle efficiency and power generation are increased. Table 4 shows a comparison between the condenser parameters during standard and repowering operation. Table 5 shows the calculated global data for the Rankine cycle in repowering operation mode. Table 6 shows the benefits of the use of the absorption chiller to the studied Rankine cycle.

Table 4. Condenser parameters comparison

Parameters	Standard mode	Repowering mode	Unit
ΔT_{ml}	9.10	8.75	[ºC]
U_c	2.50	2.50	[kW/m^2.K] (Kakaç, 2002)
$T_{condensation}$	45.00	26.63	[ºC]
Q_{rej}	47,060.40	45,237.17	[kW]
A_c	2,068.00	2,068.00	[m^2]

Table 5. Calculated global data during repowering operation

Global Data	Value	Unit		
W_{tot_gross}	32.29	[MW]		
W_{tot_net}	31.94	[MW]		
η_{cycle}	38.07	[%]		
Heat Rate	9,457.18	[MJ/MWh]		
t_S	83,730.59	[s]	23.26	[h]
t_R	2,669.41	[s]	0.74	[h]
M_{water}	2,915,291.29	[kg]		

Table 6. Main results

Main results found	Value	Unit
Net power gain	1.81	[MW]
Efficiency gain	2.16	[%]
Decrease in condenser temperature	18.37	[°C]
Daily duration of power gain	44m:29s	----

2.4.5 System optimization

In this section it is tested different mixture ratios between the cooling water from cooling tower and the cold water, cooled by the absorption chiller, to find the best ratio to increase power generation. A higher temperature mixture enables a longer period of repowering and may be beneficial. Figure 4 shows the daily energy gain according to the percentage of chilled water mixed with cooling tower water.

The graph shows that the maximum increment in energy is obtained by using 100% of chilled water for a shorter period of time instead of mixed water for a longer period. Therefore, the results previously presented correspond to the optimized ratio.

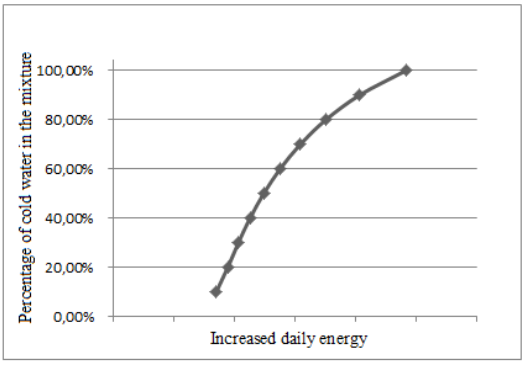

Figure 4. Energy gain according to the percentage of chilled water in the mixture

2.5 Second Proposal: Organic Rankine Cycle

In this section the ORC configurations, thermodynamic model and methodology are described. Both Recuperative ORC (RORC) and non-recuperative ORC (NORC) were tested. Supercritical conditions were used for fluids which perform better in these conditions.

2.5.1 Non-recuperative ORC

Figure 5 shows the possible configurations for the NORC with their T-s diagrams. Subcritical conditions are shown in Fig. 5(a). The fluid enters the turbine with temperature and pressure defined in state 14. Then it expands to the condensation pressure (state 15) and enters the condenser, leaving at the same pressure but as saturated liquid. This liquid is pumped to the evaporation pressure (state 17), which is lower than the critical pressure, and enters the economizer, where it is heated at constant pressure to saturated liquid state (state 24). Next, through the evaporator, the fluid evaporates and leaves as saturated vapor (state 25). If it is advantageous for the cycle the fluid is superheated next, reaching state 14. Otherwise, state 14 is the same as state 25. The heating process from state 17 to state 14 is powered by the waste heat source that goes from state 12 to state 13 as shown in Fig 5(a).

Figure 5(b) shows the supercritical configuration for the NORC. The difference between both configurations is that the fluid enters the turbine in supercritical condition. That means that the temperature and pressure of the fluid are above critical values. Therefore, the evaporation process happens directly from state 17 to state 14, above saturation line. Fluids that can operate in supercritical condition with the given heat source temperature were tested to confirm if it performs better that way.

2.5.2 Recuperative ORC

This configuration is represented in Fig. 6. The reason to use this layout is because some fluids leave the turbine after expansion as superheated vapor. The use of a recuperator allows to transfer heat from the superheated vapor to the fluid leaving the pump. The condition for applying this layout is that $T_{15}>T_{17}$. The fraction of the heat recovered is shown in Fig. 6 as area 1. This heat would originally be lost in condenser to the ambient. Like the NORC, the RORC can also be either subcritical (Fig. 6(a)) or supercritical (Fig. 6(b)) depending on the same factors exposed in Section 2.5.1.

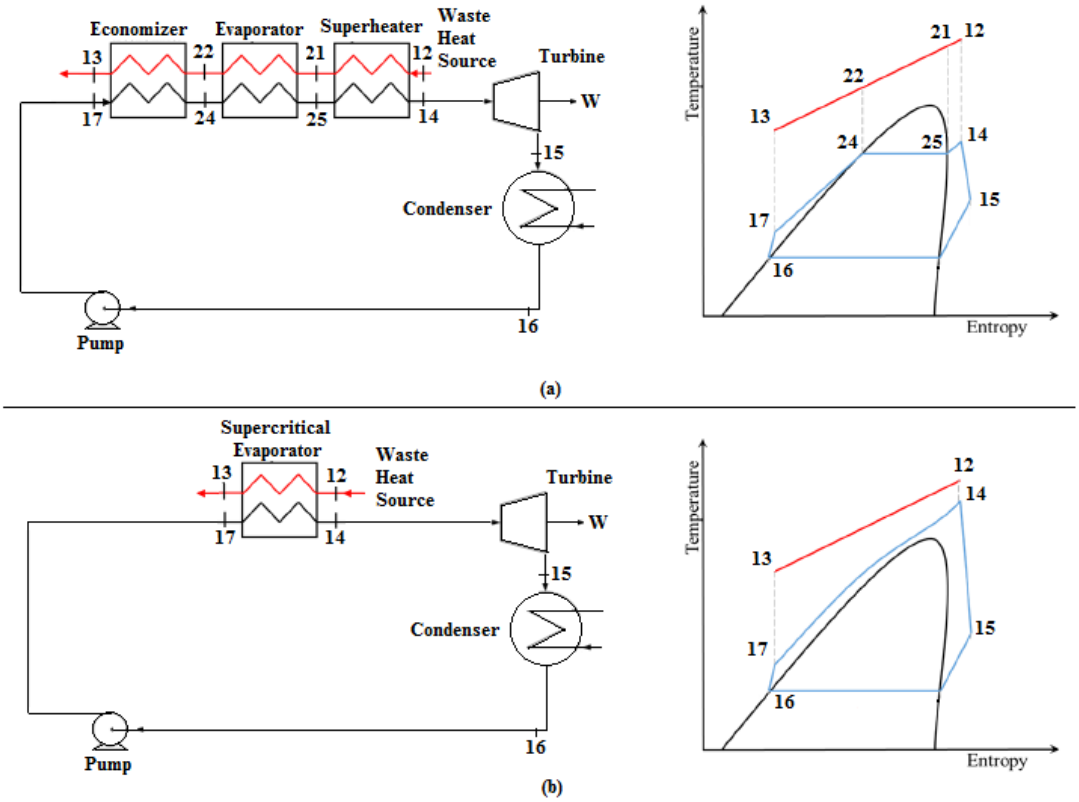

Figure 5. Configuration and T-s diagram of NORC: (a) subcritical, (b) supercritical

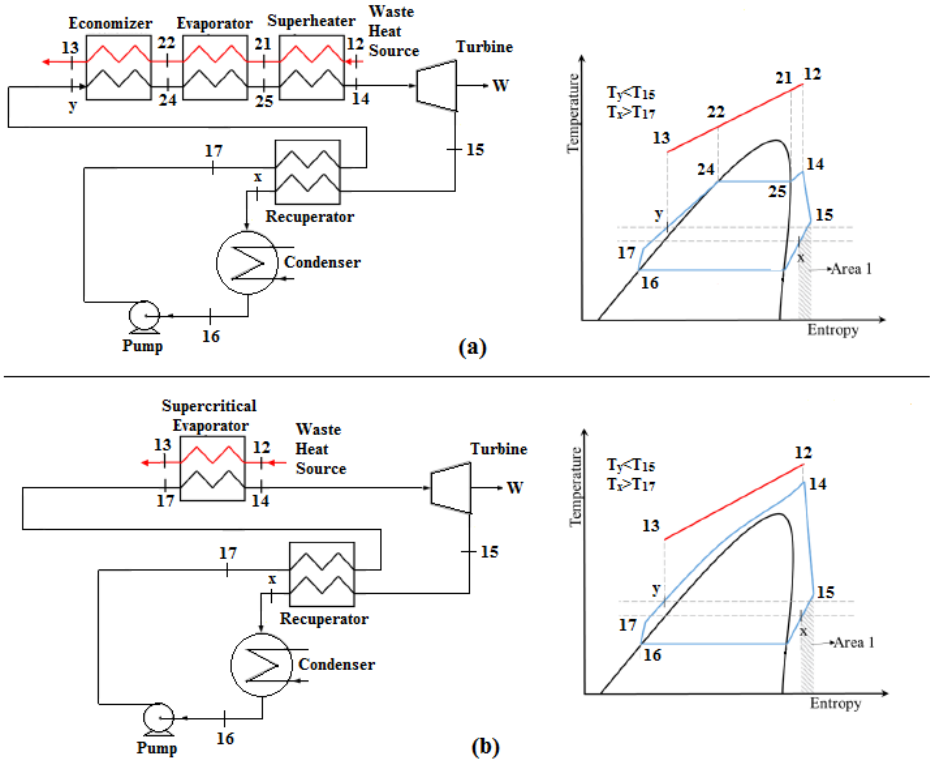

Figure 6. Configuration and T-s diagram of RORC: (a) subcritical, (b) supercritical

2.5.2 Thermodynamic model

In order to compare the results of the proposals, the heat source characteristics for the ORC are the same used for the absorption chiller. The exhaust gases mass flow rate is 35,73 kg/s at 175,61ºC. The specific heat used was the same used for the absorption chiller (1.087 $kJ.kg^{-1}K^{-1}$). The minimum temperature ate state 13 was limited to 5ºC above the acid dew point at 106,5ºC. All components were modelled at steady state and the same assumptions from section 2.1 were applied. Table 7 gives the parameters used for the simulations. Some of these parameters were set according to Mazetto et al. (2015).

Table 7. ORC Specifications for simulation

Parameter	Value	Unit
Expander isentropic efficiency ($\eta_{t,ise}$)	80	[%]
Pump isentropic efficiency($\eta_{p,ise}$)	75	[%]
Recuperator effectiveness (ε_r)	85	[%]
Pinch temperature difference at condenser	10	[ºC]
Pinch temperature difference at evaporator	10	[ºC]
Exhaust gases temperature at state 12 (T_{12})	175.61	[ºC]
Minimum temperature at state 13 (T_{13})	106.5	[ºC]
Exhaust gases mass flow rate ($\dot{m}_g$)	35.73	[kg/s]
Exhaust gases average specific heat (Cp_g)	1.087	[kJ/kgK]

Isentropic efficiencies of the expander and pump are given respectively in Eq. (8) and Eq. (9).

$$\eta_{t,ise} = \frac{h_{14} - h_{15}}{h_{14} - h_{15,ise}} \tag{8}$$

$$\eta_{p,ise} = \frac{h_{17,ise} - h_{16}}{h_{17} - h_{16}} \tag{9}$$

In these equations *h* are the specific enthalpies at the subscripted states. The energy balances for the expander and pump are given respectively in Eq. (10) and Eq. (11).

$$\dot{W}_t = \dot{m}_{wf} * (\mathrm{h}_{14} - h_{15}) \quad (10)$$

$$\dot{W}_p = \dot{m}_{wf} * (\mathrm{h}_{17} - h_{16}) \quad (11)$$

$\dot{m}_{wf}$ is the mass flow rate of working fluid. Equations (12), (13), (14) and (15) give the energy balances of the economizer, evaporator, super-heater and supercritical evaporator.

$$\dot{m}_g * Cp_{\mathrm{g}} * (T_{22} - T_{13}) = \dot{m}_{wf} * (\mathrm{h}_{24} - h_{17}) \quad (12)$$

$$\dot{m}_g * Cp_{\mathrm{g}} * (T_{21} - T_{22}) = \dot{m}_{wf} * (\mathrm{h}_{25} - h_{24}) \quad (13)$$

$$\dot{m}_g * Cp_{\mathrm{g}} * (T_{12} - T_{21}) = \dot{m}_{wf} * (\mathrm{h}_{14} - h_{25}) \quad (14)$$

$$\dot{m}_g * Cp_{\mathrm{g}} * (T_{12} - T_{13}) = \dot{m}_{wf} * (\mathrm{h}_{14} - h_{17}) \quad (15)$$

The recuperator effectiveness is defined in Eq. (16). Energy balance for this equipment is given by Eq. (17)

$$\varepsilon_r = \frac{T_{15} - T_x}{T_{15} - T_{17}} \quad (17)$$

$$h_{15} - h_x = h_y - h_{17} \quad (18)$$

The heat transferred from the exhaust gases to the working fluid is calculated by Eq. (19). Equations (20) and (21) give the net power generated and cycle efficiency.

$$\dot{Q}_H = \dot{m}_{wf} * (\mathrm{h}_{14} - h_{17}) \quad (19)$$

$$\dot{W}_{net} = \dot{W}_t - \dot{W}_p \quad (20)$$

$$\eta_{orc} = \frac{\dot{W}_{net}}{\dot{Q}_H} \quad (21)$$

2.5.3 Methodology for Optimization of the ORCs

In order to find the best configuration for the higher net power output 23 fluid candidates were tested. Table 8 shows the fluid candidates and their respective properties. The selected fluids comply with Kyoto and Montreal protocols and are the same used by Mazetto et al. (2015). The software EES® (Klein, 2015) was used to simulate the cycle. This software has a huge database of state equations and fluid thermodynamic properties and is well known in scientific media. The optimization method is the Genetic Algorithm which consists on a computational model inspired by Darwin's Theory of Evolution in search for the global optima. The optimized variables were T_{14} and P_{14}.

Table 8. Working fluid candidates properties

Substance	Type	T_{crit}(ºC)	P_{crit}(kPa)
Benzene	Dry	288.9	4894
Isobutane	Dry	134.7	3640
n-Butane	Dry	152.0	3796
n-Decane	Dry	344.6	2103
n-Dodecane	Dry	385.0	1817
n-Heptane	Dry	267.0	2727
n-Hexane	Dry	234.7	3058
n-Nonane	Dry	321.4	2281
n-Octane	Dry	296.2	2497
n-Pentane	Dry	196.5	3364
Isopentane	Dry	187.2	3370
Cyclohexane	Isentropic	280.5	4081
Toluene	Isentropic	318,6	4126
R123	Isentropic	183.7	3668

R134a	Isentropic	101.0	4059
R141b	Isentropic	204.2	4249
R142b	Isentropic	137.1	4055
R245fa	Isentropic	154.0	3651
R502	Wet	82.16	4074
R717	Wet	132.3	11330
Ethanol	Wet	241.6	6268
Propane	Wet	96.68	4247
Water	Wet	374.0	22060

2.5.4 Results

In this section the results are presented and discussed. The fluids that perform better with Non-recuperative ORC are presented in Tab. 9. The fluids that perform better with Recuperative ORC are presented in Tab. 10.

Table 9. Optimized Properties for Non-recuperative ORC

Substance	$\dot{m}_{wf}$(kg/s)	P_{14}(kPa)	T_{14}(ºC)	Condition
R502	14.24	4074	165.6	Supercritical
R717	2.623	13644	165.6	Supercritical
Ethanol	2.495	287	164.2	Subcritical
Propane	6.46	7959	165.6	Supercritical
Water	1.03	111.1	165.6	Subcritical

Table 10. Optimized Properties for Recuperative ORC

Substance	$\dot{m}_{wf}$(kg/s)	P_{14}(kPa)	T_{14}(ºC)	Condition
Benzene	5.566	236.7	120.6	Subcritical
Isobutane	7.165	4025	165.6	Supercritical
n-Butane	6.495	3796	165.6	Supercritical
n-Decane	6.576	15.42	112.9	Subcritical
n-Dodecane	6.519	3.646	113	Subcritical
n-Heptane	6.409	156.2	117.8	Subcritical
n-Hexane	6.294	369.3	118.3	Subcritical
n-Nonane	6.157	36.5	116.9	Subcritical
n-Octane	6.481	71.2	114.8	Subcritical
n-Pentane	6.614	879.1	119.8	Subcritical
Isopentane	6.876	1108	123.5	Subcritical
Cyclohexane	5.785	259.2	118.2	Subcritical
Toluene	5.798	98.2	119.8	Subcritical
R123	14.07	1063	132.7	Subcritical
R134a	14.12	6256	165.6	Supercritical
R141b	10.82	987.8	119.8	Subcritical
R142b	11.94	4109	165.6	Supercritical
R245fa	12.48	3651	165.6	Supercritical

Most substances with critical temperature lower than the waste heat source temperature reached supercritical condition. This can be explained because of the better matching of the heat source curve with the working fluid heating curve (Kalra et al., 2012). These results can be better observed in Fig. 7.

After optimizing all fluids, n-Butane presented the best results with a net power output of 409.3 kW and a cycle efficiency of 15.25%. Following comes R245fa with a 408.5 kW net power output and 15.22% efficiency. Both reached supercritical condition. The poorest results were from R502 with a power output of 102.9 kW and 3.83% efficiency. Carnot efficiency is used to evaluate how far the ORC is from thermodynamic performance upper limit. The Carnot efficiency η_{Carnot} is defined in Eq. (22).

$$\eta_{Carnot} = 1 - \frac{T_L}{T_H} \tag{22}$$

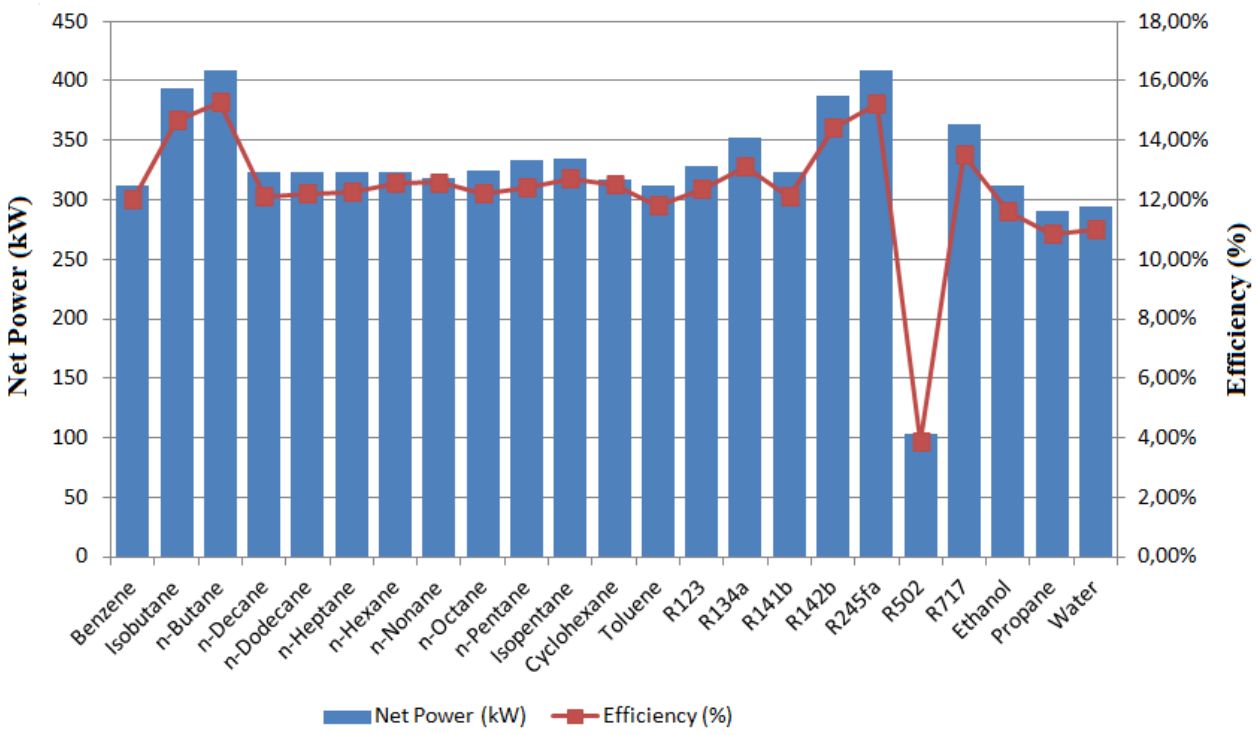

Figure 7. Optimization results

T_L is the condensation temperature, the lowest temperature of the cycle. T_H is the heat source temperature, the highest temperature of the cycle. For a T_L of 50ºC and T_L of 175.61ºC the corresponding Carnot efficiency is 27.99%. Therefore, the ORC with best results has an efficiency relative to Carnot (η_{ORC}/η_{Carnot}) of 54.38% which is a notorious result.

In next session the results from the ORC simulation are compared to the results from the absorption chiller.

2.5.5 Comparison between ORC and absorption chiller

In order to compare the results from both proposals and find the best solution it was necessary to equalize the time periods. The use of an absorption chiller resulted in a gain of 1.81 MW for a period of 2669.41s. In a daily basis that result is equivalent to an average gain of 55.92 kW which represents a gain of 0.06% in the efficiency of the studied Rankine cycle. The comparison is better represented in Tab. 11.

Table 11. Comparison between ORC and absorption chiller

Results	Abs. Chiller	ORC (n-Butane)
Net power gain (kW)	55.92	409.3
Efficiency gain (%)	0.07	0.42

3. CONCLUSION

The objective of this work was to compare two possible proposals to increase the power generated by an already existing conventional Rankine cycle. The two systems tested were an absorption chiller to cool the condenser of the cycle and an Organic Rankine Cycle, both powered by the recoverable (above dew point) waste heat from the exhaust gases from the boiler. Optimizations were conducted with 23 fluid candidates for the ORC searching for the optimal expander inlet temperature and pressure that resulted in maximum net power generation.

The absorption chiller increased the power output in 1.81 MW for a period of 44 minutes and 29 seconds, which represents a daily average gain of 55.92 kW. The Recuperative ORC with n-Butane represented a gain of 409.3 kW in net power generation under the optimized conditions shown in Tab. 10.

These results indicate that thermodynamically it is more advantageous to fit an ORC to the Rankine Cycle studied because it results in a higher gain in power generated. Further studies need to be conducted in order to compare the economical benefits of both systems.

4. ACKNOWLEDGEMENTS

Vitor R. Seifert gratefully acknowledges the Industrial Engineering Program, Federal University of Bahia. This author also acknowledges FAPESB (Fundação de Amparo ao Pesquisador do Estado da Bahia) for the provision of master scholarship. Ednildo A. Torres would like to thank the National Council for Scientific and Technological Development (CNPq).

5. REFERENCES

Agnew, B., Alaktiwi, A., Anderson, A., Potts, I., 2004. "Simulation of a combined Rankine-aborption cycle". Journal Applied Thermal Engineering, Vol. 24, pp. 1501-1511.

Battistam, D., Mauriello, M., Cipollone, R., 2015. "Waste heat recovery for an ORC-based power unit in a turbocharged diesel engine propelling a light duty vehicle". Applied Energy, Vol. 152, pp. 109-120.

Calise, F., D'accadia, M., Vicidomini, M., Scarpellino, M., 2015. "Design and simulation of a prototype of a small-scale solar CHP system based on evacuated flat-plate solar collectors and Organic Rankine Cycle". Energy Conversion and Management, Vol. 90, pp. 347-363.

Camporeale, S., Pantaleo, A., Ciliberti, P., Fortunato, B., 2015. "Cycle configuration analysis and techno-economic sensitivity of biomass externally fired gas turbine with bottoming ORC". Energy Conversion and Management, Vol. 105, pp. 1239-1250.

Celis, C., Avellar, V. P., Ferreira, S. B., 2007. "Evaluation of different alternatives of power augmentation for an existing combined cycle power plant in Brazil". Journal of Power for Land, Sea and Air. (ASME), pp. 1-10.

Chacartegui, R., Sánchez, D., Muñoz, J., Sánches, T., 2009. "Alternative ORC bottoming cycles for combined cycle power plants". Applied Energy, Vol. 86, pp. 2162-2170.

Chacartegui, R., Becerra, J., Blanco, M., Muñoz-Escalona, J., 2015. "A Humid Air Turbine-Organic Rankine Cycle combined cycle for distributed microgeneration". Energy Conversion and Management, Vol. 104, pp. 115-126.

Clemente, S., Micheli, D., Reini, M., Taccani, R., 2013. "Bottoming organic Rankine cycle for a small scale gas turbine: A comparison of different solutions". Applied Energy, Vol. 106, pp. 355-364.

Galindo, J., Ruiz, S., Dolz, V., Royo-Pascual, L., Haller, R., Nicolas, B., Glavatskaya, Y., 2015. "Experimental and thermodynamic analysis of a bottoming Organic Rankine Cycle (ORC) of gasoline engine using swash-plate expander. Energy Conversion and Management, Vol. 103, pp. 519-532.

Ganapathy, V., 1994. Steam Plant Calculations Manual. 2nd ed., rev. and expanded. ABCO Industries. Abilene, Texas, USA.

Kakaç, S., LIU, H. 2002. Heat Exchangers. Selection, Rating and Thermal Design. New York: CRC Press.

Kalra, C., Becquin, G., Jackson, J., Laursen, A. L., Chen, H., Myers, K., Klockow, H., Zia, J., 2012. "High-potential working fluids and cycle concepts for next-generation bynary organic rankine cycle for enhanced geothermal systems". Thirty-Seventh Workshop on Geothermal Reservoir Engineering. Stanford, USA.

Kim, T.S. and Ro, S.T., 2000. "Power augmentation of combined cycle power plants using cold energy of liquefied natural gas". Journal of Energy, Vol. 25, pp. 841-856.

Klein, S.A. Engineering Equation Solver (EES), Academic Professional V9.901, 2015.

Mazetto, B., Silva, J., Oliveira Jr., S., 2015. "Are ORCs a Good Option for Waste Heat Recovery in a Petroleum Refinery?". International Journal of Thermodynamics, Vol. 18, pp. 161-169.

Munõz, J., Martínez-Val, J.M., Abbas, R., Abánades, A. 2012. "Dry cooling with night cool storage to enhance solar power plants performance in extreme conditions areas". Journal of Applied Energy, Vol. 92, pp. 429-436.

Rahbar, K., Mahmoud, S., Al-Dadah, R., Moazami, N., 2015. "Modeling and optimization of organic Rankine cycle based on a small-scale radial inflow turbine". Energy Conversion and Management, Vol. 91, pp. 186-198.

Shirazi, A., Najafi, B., Aminyavari, M., Rinaldi, F., Taylor, R. A. 2014. "Thermal-economic-environmental analysis and multi-objective optimization of an ice thermal energy storage system for gas turbine cycle inlet air cooling". Journal of energy, pp. 1-15.

Shu, G., Gao, Y., Tian, H., Wei, H., Liang, X., 2014. "Study of mixtures based on hydrocarbons used in ORC (Organic Rankine Cycle) for engine waste heat recovery". Energy, Vol. 74, pp. 428-438.

Song, J., Song, Y., Gu, C., 2015. "Thermodynamic analysis and performance optimization of an Organic Rankine Cycle (ORC) for engine waste heat recovery". Energy, Vol. 82, pp. 976-985.

5. RESPONSIBILITY

The authors are the only responsible for the printed material included in this paper.